Fault Tolerant Control Design for a Tidal Current Turbine Generation System

Author Name(s): Xuhua Yan, Rosemary Norman, Mohammed Elgendy
School of Engineering, Newcastle University.
Newcastle Upon Tyne, UK

ABSTRACT

Tidal energy is renewable and also highly predictable however, access for maintenance operations on devices is limited and very expensive. The immense forces impacting on tidal current turbines (TCT) may cause component failures which have the potential to result in loss of power generation. Fault tolerant control offers the potential for the TCT to continue operating in the event of failures in components such as tidal velocity sensors. This paper presents a fault tolerant control methodology for maximum power point tracking in the event of a tidal velocity sensor failure with simulation results demonstrating the capability of the technique.

KEY WORDS: Fault tolerant control; tidal current turbine; robustness; P&O; PMSG; MPPT

INTRODUCTION

Renewable energy is making a greater contribution than ever in supplying global energy demand. Due to the predictability and capacity of the tidal currents, the position of tidal energy in the renewable energy mix has significantly increased with tidal current energy starting to make contribution (Benbouzid et al., 2011).

Tidal current turbines capture energy from tidal currents using technology which is very similar to the wind turbine capture of energy from moving air (Clarke et al., 2006). The water density is significantly higher than that of the air, so tidal current turbines operate at lower speeds but higher torques compared with wind turbines. In tidal current turbine systems, there is the potential for certain faults to cause failure of the whole system because the devices are subjected to large forces from strong tidal currents. Such failures would generally require retrieval of the device to carry out maintenance on shore but the time window to access a device is limited both by the weather and the tidal currents themselves (Sousounis et al., 2016). In order to reduce the maintenance time and increase the energy capture, fault tolerant control is essential in tidal current turbine systems.

Fig. 1 shows the percentage breakdown of failures that occurred during the period 2000-2004 in Swedish wind power plants, from this figure it can be seen that the sensor faults accounted for 14.1%, faults in electric systems 17.5% and faults in control system 12.9%. These are the most common faults that might occur in the electrical side of the system (Amirat et al., 2009). The electrical control system of a tidal current turbine is sufficiently similar to that of the wind turbine for the fault data of wind turbines to be considered as a reference for tidal current turbines.

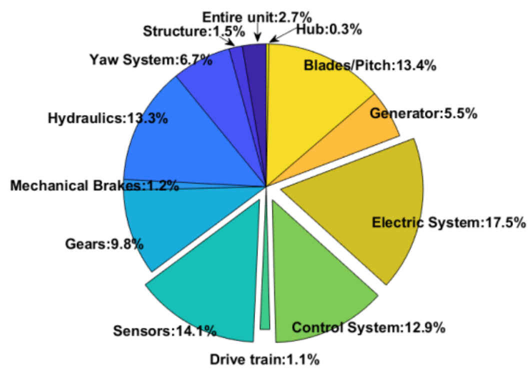

Fig. 1 Occurrence (%) of failures for Swedish wind power plants between 2000-2004.

In this paper, the sensor faults on the electrical side will be briefly introduced, as well as some corresponding potential solutions. The fault that this paper focuses on is the tidal current speed sensor fault. Generally, the sensor faults that occur in tidal current turbine systems are tidal current speed sensor faults and generator rotor speed faults. The tidal current speed sensors are often lost or damaged due to the underwater environment and strong tidal currents (Pham et al., 2017). Rotor speed sensors are generally installed on the rotor shaft; the accuracy of this kind of mechanical sensor will be influenced by environment factors, such as humidity, temperature and vibration, all of which will be significant in the underwater turbines and will potentially cause problems with the speed readings (Pham et al., 2015).

This paper will present a basic control structure for a tidal current turbine generation system with a Permanent Magnet Synchronous Generator (PMSG), the control of the tidal current turbine system is achieved by using maximum power point tracking (MPPT) to extract the maximum power, and proportional integral (PI) regulators to control the speed and *dq*-axis current.

The paper is structured as follows: potential solutions for tidal current speed sensor faults will be introduced first. Then a typical control strategy of a tidal current turbine system will be illustrated. Basic on this conventional control strategy, a fault tolerant control methodology dealing with tidal current speed sensor faults is presented that uses the Perturb and Observe (P&O) control algorithm, and results will be shown and discussed. All of the models are simulated in MATLAB/Simulink.

TIDAL CURRENT TURBINE MODELLING

The power that a turbine can extract from the tidal current can be expressed by:

$$P_t = \frac{1}{2} C_p(\lambda, \beta) \rho \pi R^2 V^3 \tag{1}$$

where the P_t is the turbine power (W), R is the radius of the turbine blades (m) and C_p is the power coefficient, which is approximated as a function of the turbine blades' pitch angle β and the tip-speed ratio λ, the water density ρ (kgm^{-3}) and the tidal flow velocity V (ms^{-1}) (Ghefiri et al., 2017). Generally if the turbine is a fixed pitch device, the value of β is constant and equals 0. The tip-speed ratio λ is defined by

$$\lambda = \frac{\omega_r R}{V} \tag{2}$$

where the ω_r is the angular speed of the rotor (rad/s).

From Eq. 1 can be seen that the power P_t is proportional to the power coefficient C_p, and from Eq. 2, the tip-speed ratio λ is proportional to rotor speed ω_t. In order to get the maximum power from the turbine, as it can be seen from Fig. 2, the turbine must operate at one specific value of λ. This means, that to improve the energy capture from the turbine, the rotor speed must be adjusted to make sure that C_p can reach the maximum value. For different tidal current turbine systems the specific values of C_p and λ will be different but Fig. 2 is representative of a typical characteristic.

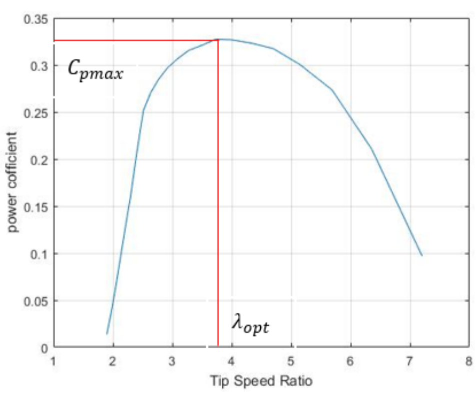

Fig. 2 Tidal current turbine power coefficient with respect to the tip speed ratio

TIDAL CURRENT GENERATOR MODELLING

The generator that was used in this work is a PMSG, and the fault tolerant control strategy that is presented is based on the PMSG. Compared with other generators, PMSG have the advantage of higher efficiency, higher power density and better grid compatibility (Zhao et al., 2013), all factors which make them suitable for use in tidal current turbines.

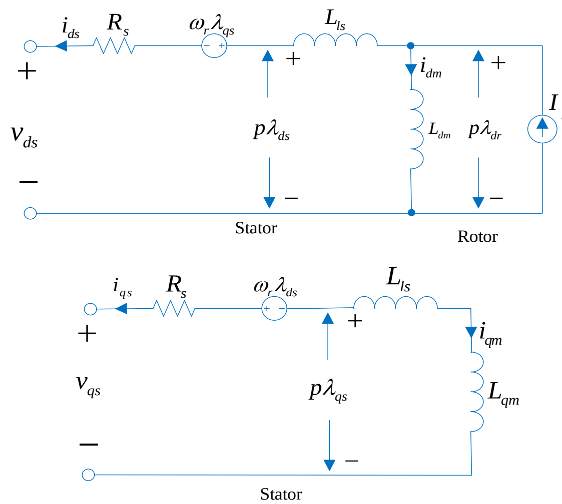

Fig. 3 PMSG *dq* equivalent circuit (Toumi et al., 2017)

Fig. 3 shows a model of the PMSG as a *dq*-axis equivalent circuit. From the equivalent circuit, the voltage equations of the PMSG in the *dq*-axis form can be expressed as follows (Wu et al., 2011):

$$v_{ds} = -R_s i_{ds} - \omega_r \lambda_{qs} + \frac{d\lambda_{ds}}{dt} \tag{3}$$

$$v_{qs} = -R_s i_{qs} + \omega_r \lambda_{ds} + \frac{d\lambda_{qs}}{dt} \tag{4}$$

Where i_{ds} is d-axis stator current, i_{qs} is q-axis stator current, v_{ds} is d-axis stator voltage, v_{qs} is q-axis stator voltage, R_s is the winding (stator) resistance (Ω), ω_r is the electrical rotational speed (rad/s) and λ_{qs} and λ_{ds} are dq-axis stator flux (Wb) which can be defined as follows (Wu et al., 2011):

$$\lambda_{ds} = -L_d i_{ds} + \lambda_r \tag{5}$$

$$\lambda_{qs} = -L_q i_{qs} \tag{6}$$

L_d and L_q are the winding (stator) inductances (H), λ_r is the rotor (permanent magnet) flux (Wb). Substituting Eqs. (5) and (6) into (3) and (4) gives:

$$v_{ds} = -R_s i_{ds} + \omega_r L_q i_{qs} - L_d \frac{di_{ds}}{dt} \tag{7}$$

$$v_{qs} = -R_s i_{qs} - \omega_r L_d i_{ds} - L_q \frac{di_{qs}}{dt} + \omega_r \lambda_r \tag{8}$$

Rearranging the *dq*-axis voltage Eqs. (7) and (8) gives the dq-axis current equations:

$$\frac{di_{ds}}{dt} = -\frac{R_s}{L_d} + \frac{L_q}{L_d} \omega_r i_{qs} + \frac{v_{ds}}{L_d} \tag{9}$$

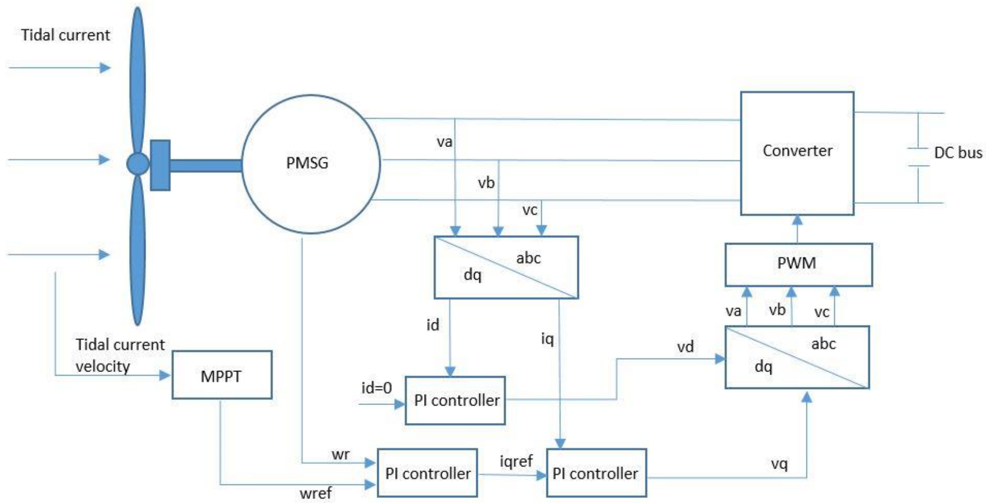

Fig. 4 Typical tidal current turbine system control structure

$$\frac{di_{qs}}{dt} = -\frac{R_s}{L_q} i_{qs} - \frac{1}{L_q}\omega_r(L_d i_{ds} + \lambda_r) + \frac{v_{qs}}{L_q} \quad (10)$$

The electromagnetic torque is then given by:

$$T_e = \frac{3}{2}p(i_{qs}\lambda_{ds} - i_{ds}\lambda_{qs}) \quad (11)$$

Where p is the number of pole pairs. Substituting Eqs. (5) and (6) into (11) gives:

$$T_e = \frac{3}{2}p[i_{qs}\lambda_r - (L_d - L_q)i_{ds}i_{qs}] \quad (12)$$

Fig. 4 shows a typical tidal current turbine generation system control structure; the fault tolerant control strategies are developed based on this structure. The system generally consists of MPPT control, a speed PI controller, and two current PI controllers, *abc/dq* and *dq/abc* conversions, and a PWM rectifier. MPPT in this system is used to provide a reference speed from the tidal current speed sensor to maximise the power coefficient and the MPPT algorithm is:

$$\omega_{ref} = \frac{\lambda_{opt}V}{R} \quad (13)$$

where λ_{opt} is the value of tip-ratio speed that corresponds to the maximum power coefficient, C_p, as shown in Fig. 2.

TIDAL CURRENT SPEED SENSOR FAULT TOLERANT CONTROL

Tidal current turbines need to be installed at locations with strong tidal current, so that maximum power can be captured. In such situations, the tidal current speed sensors (flow-meter) are often lost or damaged. The reading of tidal current is used to calculate the reference speed within the MPPT unit in order to make sure that the tip-speed ratio is around the optimal value. To avoid the potential problems with the tidal current speed sensor, a fault tolerant control strategy can enable the system to achieve continuous operation without the reading of tidal current (Pham et al., 2017). This section will give an introduction to the tidal current speed sensor fault tolerant control.

Power signal feedback control

The maximum power that a tidal current turbine can capture can be expressed as follows (Zhao et al., 2013):

$$P_{max} = \frac{C_{pmax}\rho\pi R^5}{2\lambda_{opt}^3}\omega_r^3 = K_{opt}\omega_r^3 \quad (14)$$

Where C_{pmax} is the maximum power coefficient when the tip speed ratio is at its optimal value (λ_{opt}). Thus, the rotor speed reference can be calculated as follows (Pham et al., 2017):

$$\omega_r^* = \sqrt[3]{\frac{P_{max}}{K_{opt}}} \quad (15)$$

Fig. 5 shows the block diagram of the power signal feedback control in which the reference speed is used to adjust the generator speed to its optimal value by using Eq. 15, so that the tidal current turbine power can converge to the maximum value under a specific tidal current condition.

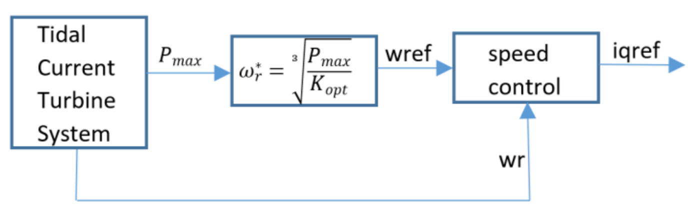

Fig. 5 Power signal feedback control diagram

Optimal torque control

The optimal torque control is similar to the power signal feedback control, but the generator needs to be controlled in torque control mode. Since $P = \omega * T$, the optimal torque can be expressed as (Zhao et al., 2013):

$$T_{opt} = \frac{C_{pmax}\rho\pi R^5}{2\lambda_{opt}^3}\omega_r^2 = K_{opt}\omega_r^2 \quad (16)$$

The rotor speed is used to calculate the reference optimal torque which is used to adjust the turbine torque through an optimal torque curve. The

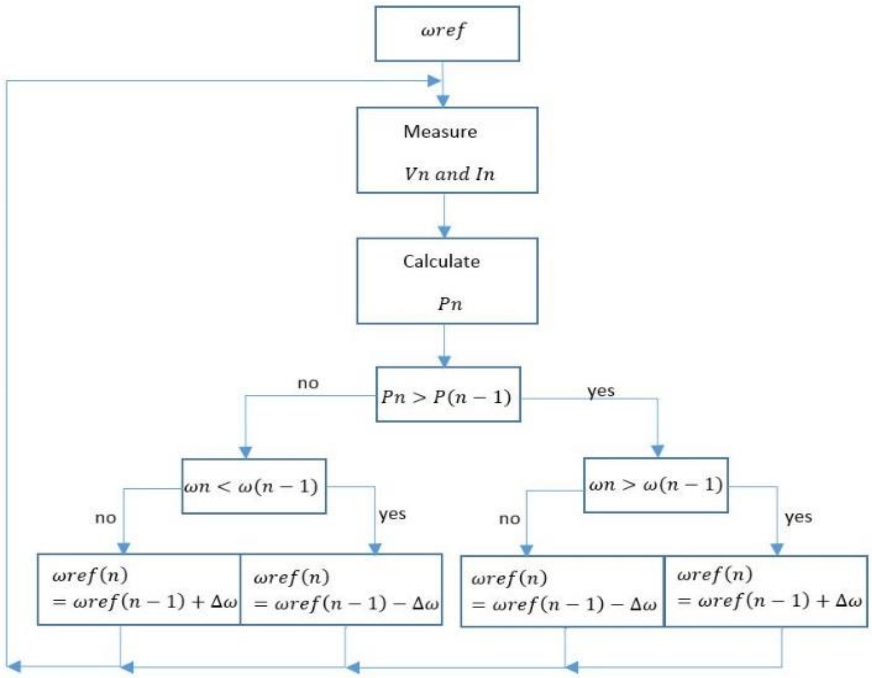

Fig. 7 P&O control flow chart

block diagram of OT control is illustrated in Fig. 6 (Zhao et al., 2013).

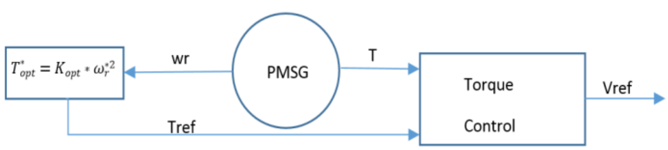

Fig. 6 Optimal torque control diagram

Perturbation- Observation control

Perturbation-Observation (P&O) control does not rely on the tidal current speed information and tidal current turbine characteristics. The theory of P&O control is to create a change in generator speed and observe the corresponding changes in power. This is the fault tolerant control strategy that used in this paper. Fig. 7 is the control flow chart and Fig. 8 is the control diagram.

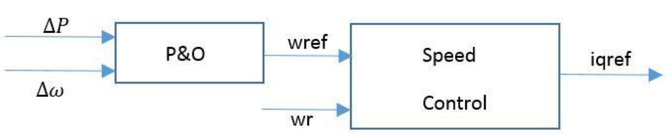

Fig. 8 P&O control diagram

During the searching process, the P&O control continuously gives the generator reference speed, and the control system adjusts the actual generator speed to follow this reference. The reference speed is increased or decreased by $\Delta\omega$ in each step. In the tidal current turbine generation system, the output voltage is proportional to the generator speed, so the change in generator speed leads to a change in output power by ΔP. If $\Delta P > 0$, the search direction in next step is the same, if $\Delta P < 0$, then the search direction is opposite. Fig. 9 shows the searching process.

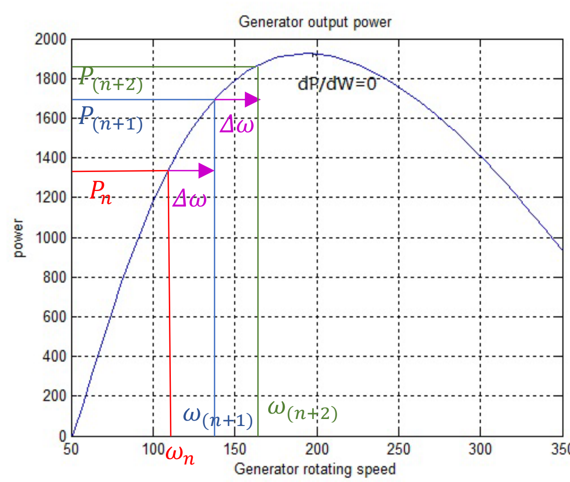

Fig. 9 P&O control searching process

TIDAL CURRENT TURBINE GENERATION SYSTEM WITH P&O CONTROL

As mentioned in the above sections, this paper will present a tidal current turbine generation system with P&O control to deal with tidal current speed sensor failures. This system can operate without the tidal current speed sensor, and can track the maximum power point, ensuring that the turbine works near the MPP.

System modelling

According to the power coefficient versus tip speed ratio figure (Fig. 2) and turbine power extraction equation (Eq. 1) in this particular case has a relationship between the power coefficient C_p and tip speed ratio λ as follows:

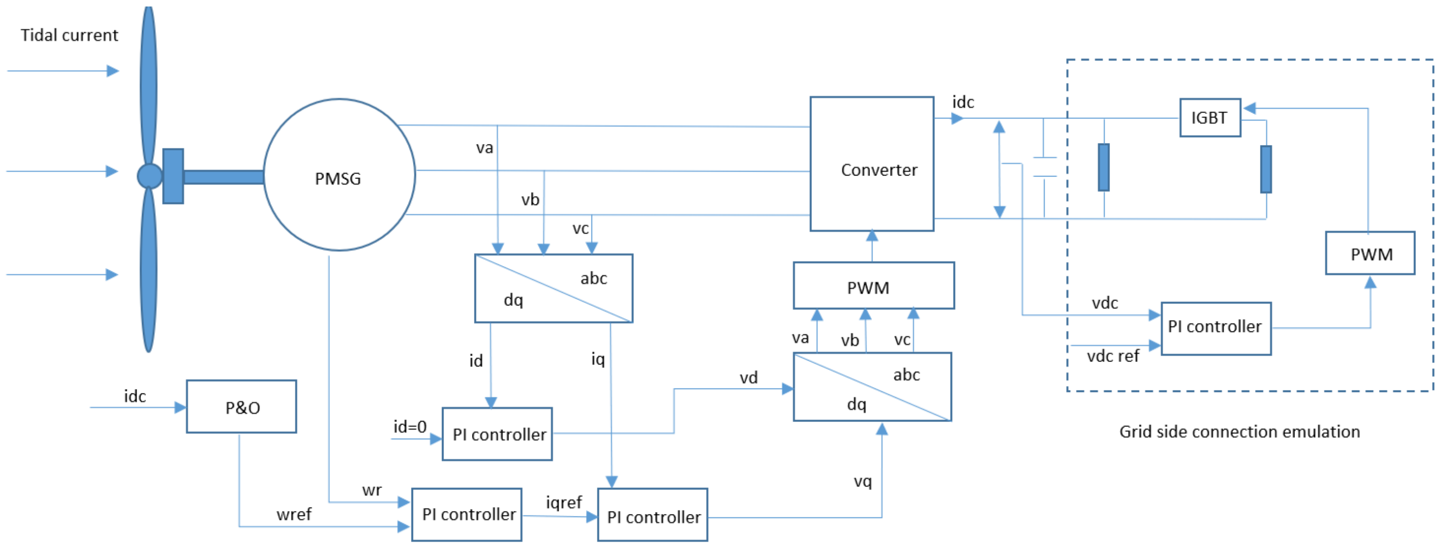

Fig. 10 Tidal current turbine generation system with P&O control

$$C_p = 0.001161\lambda^5 - 0.030582\lambda^4 + 0.3139\lambda^3 - 1.5888\lambda^2 + 3.976\lambda - 3.6047 \quad (28)$$

When $\frac{dC_p}{d\lambda} = 0$, the power that the turbine captures is the maximum value; from the calculation, $C_{pmax} = 0.3294$ and $\lambda_{opt} = 3.774$.

In the full system model for a tidal current turbine, the DC-link voltage is the input to a grid side converter which controls the power of the whole system. In this paper, in order to focus on the P&O control, the system is simplified to have the DC-link voltage through an IGBT switch, so that the DC-link voltage is stable. The system block diagram is illustrated in Fig. 10. This system is simulated in MATLAB/Simulink based on Fig. 10. Based on Fig. 7 and Fig. 8, the P&O control model is simulated as shown in Fig. 11

In the model, the input of the system is tidal current speed, it is set as 1.9m/s and then a step change to 2.1m/s happens at 25s of simulation time. This is to illustrate the control operation although in reality the tidal current speed would change more gradually.

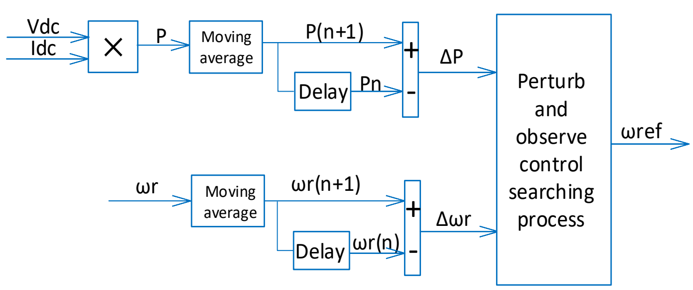

Fig. 11 P&O control model

The moving average functions shown in Fig. 11 are used to calculate the average values of power and generator speed, removing the effects of the power converter switching. As illustrated in Fig. 7, the P&O control use the change of power and generator rotor speed as inputs, and according to the changes in power and rotor speed, it controls the rotor reference speed. The reference speed is the input of the generator side converter control, then the system adjusts the generator speed to converge to the reference speed.

Results

Simulation results of the tidal current turbine generation system with P&O fault tolerant control are presented in the following figures.

Fig. 12 shows the generator rotor reference speed which is also the output of the P&O control, the generator side converter control will regulate the generator rotor speed to follow the reference speed, so that the turbine will operate in the optimal tip-speed ratio range. It can be seen from Fig. 12 that the P&O control is a three-level operation, and it is also a variable step size algorithm. The step size is smaller when the reference speed is near the optimal value than it is in the searching process. The chosen of P&O step size and perturbation period will influence the response of the system. A big step size will make the control algorithm track the optimal value quickly but when the system reaches the steady state, the speed will fluctuate over a large range, and may make the speed PI controller unstable. A small step size will take more time for the system to reach steady state, but the system will be more stable during the steady state. The perturbation period cannot be smaller than the system response time, otherwise the system will never reach the steady state. Fig.12 shows that the reference value tracks the calculated theoretical value within an acceptable range.

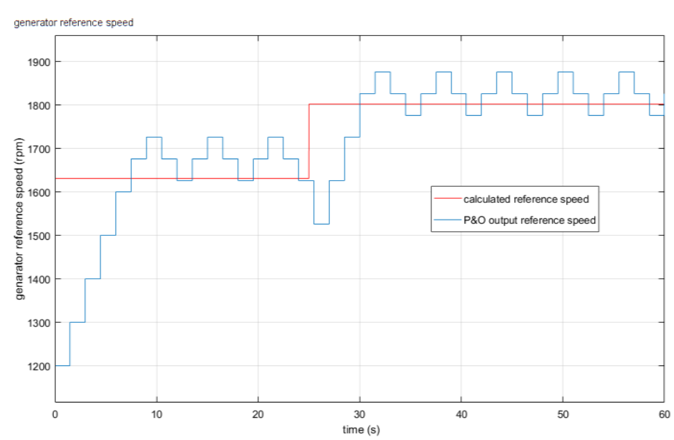

Fig. 12 Generator rotor reference speed (output of P&O control)

Fig. 13 illustrates that the tidal current turbine power coefficient value; the real power coefficient, is very close to the maximum value, and it is clear that the turbine coefficient is close to the maximum value and oscillates over a small range near the maximum value. This means that the power that is captured by the tidal current turbine is near the optimal value and this is the aim of MPPT algorithm.

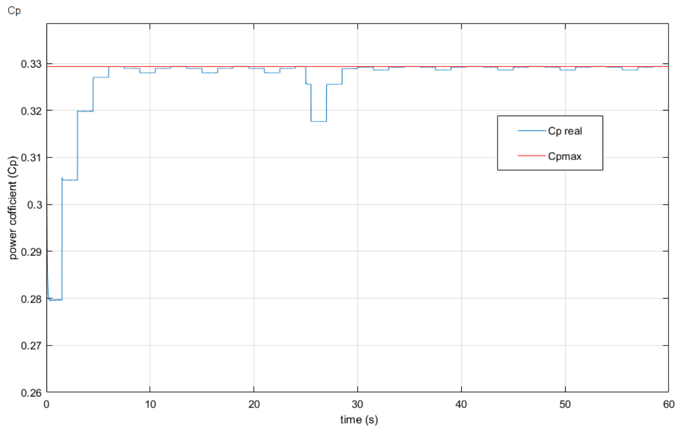

Fig. 13 Tidal current turbine power coefficient

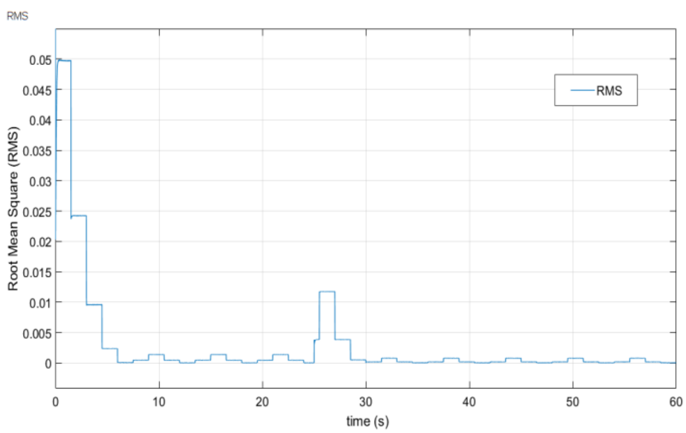

Fig. 14 Root-Mean-Square (RMS) of power coefficient (Cp)

In Fig. 14 the Root-Mean-Square (RMS) error of the turbine power coefficient is presented and it can be seen that the error is very small and would be in an acceptable range.

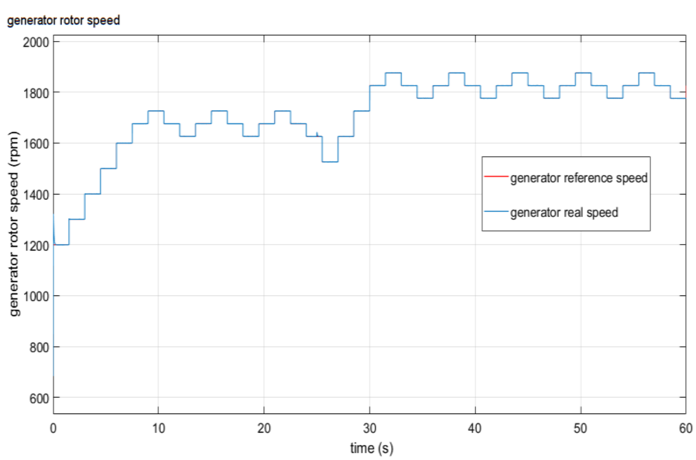

Fig. 15 Generator rotor speed

Fig. 15 shows the generator rotor speed; as mentioned above, the generator rotor speed is controlled by the generator side convertor to converge to the generator reference speed. Fig. 16 shows a zoomed in view of the rotor speed, demonstrating that the generator is able to follow the reference speed changes rapidly and it is stable during the steady state. This means that the P&O control step size and perturbation period are acceptable for the system control strategy. Fig.17 illustrates the DC link voltage, which is controlled to be stable. The value of DC voltage depends on the load resistance value and the generator rated power. The DC voltage could also be controlled by a grid side convertor, which means that this system can be used for grid connection.

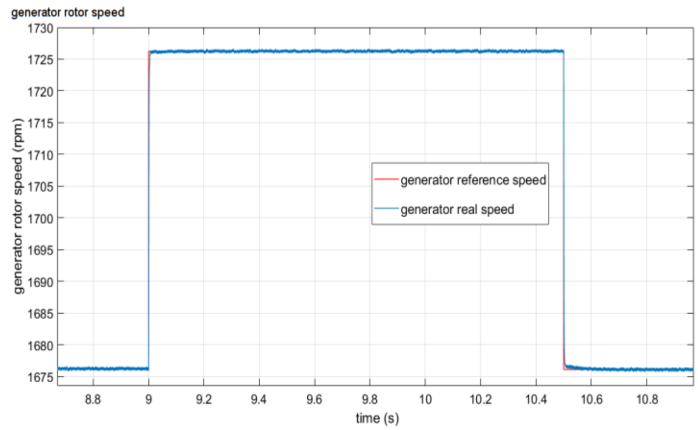

Fig. 16 Zoomed in view of the generator rotor speed

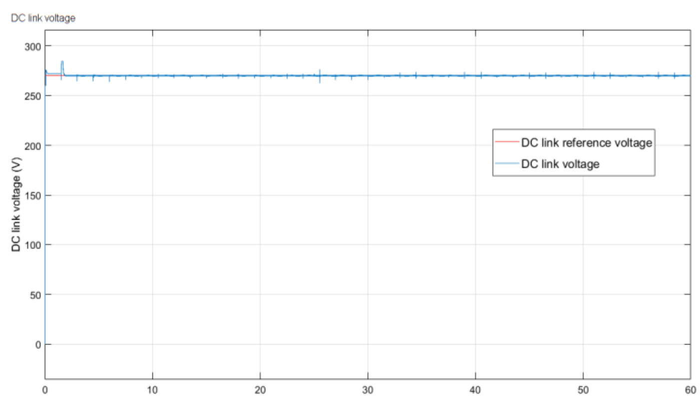

Fig. 17 DC-link voltage

CONCLUSION

In this paper, some fault tolerant control methods are brief introduced, and a conventional tidal current turbine generation system is presented. The system model is simulated based on MATLAB/Simulink. In order to deal with a tidal current speed sensor fault, the maximum power point tracking has been developed based on P&O control. The results of the model simulation have illustrated that in the conventional tidal current turbine generation system, the P&O based MPPT can track the maximum power point effectively without a reading from a tidal current speed sensor, and this system can have a grid side converter added so that it can be applied in a grid connection mode. For future work, some other control methods can be developed in the conventional system to solve additional sensor faults.

REFERENCES

Amirat, Y., Benbouzid, M., Al-Ahmar, E., Bensaker, B., & Turri, S. (2009). A brief status on condition monitoring and fault diagnosis in wind energy conversion systems. Renewable and Sustainable Energy Reviews, 13(9), 2629–2636.

Benbouzid, M., Astolfi, J. A., Bacha, S., Charpentier, J. F., Machmoum, M., Maitre, T., & Roye, D. (2013). Concepts, Modeling and Control of Tidal Turbines. Marine Renewable Energy Handbook, 219–278.

Clarke, J.A., Connor, G., Grant, A.D. and Johnstone, C.M. (2006) 'Regulating the output characteristics of tidal current power stations to facilitate better base load matching over the lunar cycle', Renewable Energy, Vol. 31, No. 2, pp.173–180.

Ghefiri, K., Bouallègue, S., Garrido, I., Garrido, A., & Haggège, J. (2017). Complementary Power Control for Doubly Fed Induction Generator-Based Tidal Stream Turbine Generation Plants. Energies, 10(7), 862.

Pham, H.-T., Bourgeot, J.-M., & Benbouzid, M. E. H. (2017). Comparative Investigations of Sensor Fault-Tolerant Control Strategies Performance for Marine Current Turbine Applications. IEEE Journal of Oceanic Engineering, 43(4).

Pham, H.-T., Bourgeot, J.-M., & Benbouzid, M. (2015). Performance comparison of sensor fault-tolerant control strategies for PMSG-based marine current energy converters. IECON 2015 - 41st Annual Conference of the IEEE Industrial Electronics Society.

Sousounis, M. C., Shek, J. K., & Mueller, M. A. (2016). Modelling, control and frequency domain analysis of a tidal current conversion system with onshore converters. IET Renewable Power Generation, 10(2), 158-165.

Toumi, S., Benelghali, S., Trabelsi, M., Elbouchikhi, E., Amirat, Y., Benbouzid, M., & Mimouni, M. F. (2017). Modeling and Simulation of a PMSG-based Marine Current Turbine System under Faulty Rectifier Conditions. Electric Power Components and Systems, 45(7), 715–725.

Wu, B., Lang, Y., Zargari, N., & Kouro, S. (2011). Power conversion and control of wind energy systems (Vol. 76). John Wiley & Sons.

Zhao, Y., Wei, C., Zhang, Z., & Qiao, W. (2013). A Review on Position/Speed Sensorless Control for Permanent-Magnet Synchronous Machine-Based Wind Energy Conversion Systems. IEEE Journal of Emerging and Selected Topics in Power Electronics, 1(4), 203–216.